

See discussions, stats, and author profiles for this publication at: <https://www.researchgate.net/publication/231653856>

Role of Coverage and Surface Oxidation Degree in the Adsorption of Acetone on TiO₂ (110). A Density Functional Study

ARTICLE in THE JOURNAL OF PHYSICAL CHEMISTRY C · NOVEMBER 2009

Impact Factor: 4.77 · DOI: 10.1021/jp906643h

CITATIONS

13

READS

14

3 AUTHORS:



Antonio Márquez

Universidad de Sevilla

84 PUBLICATIONS 1,348 CITATIONS

[SEE PROFILE](#)



Jose j. Plata

Duke University

22 PUBLICATIONS 236 CITATIONS

[SEE PROFILE](#)



Javier Fdez Sanz

Universidad de Sevilla

62 PUBLICATIONS 1,631 CITATIONS

[SEE PROFILE](#)

Role of Coverage and Surface Oxidation Degree in the Adsorption of Acetone on TiO₂ (110). A Density Functional Study

Antonio M. Márquez,* José J. Plata, and Javier Fdez. Sanz

Departamento de Química Física, Universidad de Sevilla, Facultad de Química, CL/Prof. García González 1, 41012 Sevilla, Spain

Received: July 14, 2009; Revised Manuscript Received: September 18, 2009

A systematic study of the adsorption of acetone on a TiO₂ (110) surface by means of plane-wave pseudopotential density-functional theory calculations is presented. The relationship between the binding energy of acetone and the degree of surface coverage (up to 0.5 ML) is established on the basis of a partial reduction of the surface by the incoming acetone molecules. This allows one to explain the observed displacement toward lower temperature of the temperature-programmed desorption (TPD) maximum with increasing acetone loading. Adsorption at the bridge oxygen vacancies on supercell models of the reduced surface shows similar properties to that of regular Ti channel sites, in agreement with experimental data that do not indicate a preferential binding at vacancy sites. A high dependency between the degree of reduction of the surface and the acetone binding energies is found, implying that surface models with an excessive mean number of vacancies per unit cell may result in altered properties of this surface. Models of the oxidized TiO₂ (110) surface show that coadsorbed oxygen stabilizes acetone via the formation of acetone/O-adatom complexes that, in contrast to acetone, present a barrier for desorption. This barrier allows one to explain the high temperature feature observed in the TPD spectrum for acetone desorption from the oxidized TiO₂ (110) surface.

Introduction

Titanium dioxide has received considerable attention in the literature due to its utility as a catalyst and as a photocatalyst. In particular, the rutile TiO₂ (110) surface has become a prototype system in surface science studies of metal oxide surfaces.^{1–5}

The (110) surface of rutile TiO₂ is composed of alternating rows of 2-fold coordinated bridging O_b atoms and channels that expose both 5-fold coordinated Ti and in-plane 3-fold coordinated atoms (see Figure 1). Bridging oxygens have attracted an enormous interest because they can be easily removed by annealing the TiO₂ (110) surface in vacuum at temperatures about 800 K. The presence of these vacancies has been detected with a variety of techniques, and typical experiments quantify their concentration as 7%–10%.^{5,6} The reactivity of this reduced surface is largely dominated by these point defect sites as has been shown by several experimental and theoretical studies.^{1,3,4,7–10}

The interaction of O₂ with reduced TiO₂ surfaces is strong and leads to irreversible dissociation, producing surfaces with excess oxygen that show a complex O₂–TiO₂(110) chemistry.^{11–14} The simultaneous presence of water on these surfaces, even in ultrahigh vacuum (UHV) experiments, as has been recognized by several studies,^{15–18} makes the situation highly complex as different species can coexist on the surface.

Data from temperature-programmed desorption (TPD) experiments and from electron energy loss spectroscopy (EELS) demonstrate that both molecular and dissociative forms of O₂ exist on the TiO₂ (110) surface.^{13,14} Adsorption of an O₂ molecule at a vacancy site results, at least, on one dissociative channel that fills the vacancy with an O atom and deposits the second O atom on the surface channels. These O adatoms have been detected using STM and have been found to be specially reactive toward some probe molecules. These is also evidence

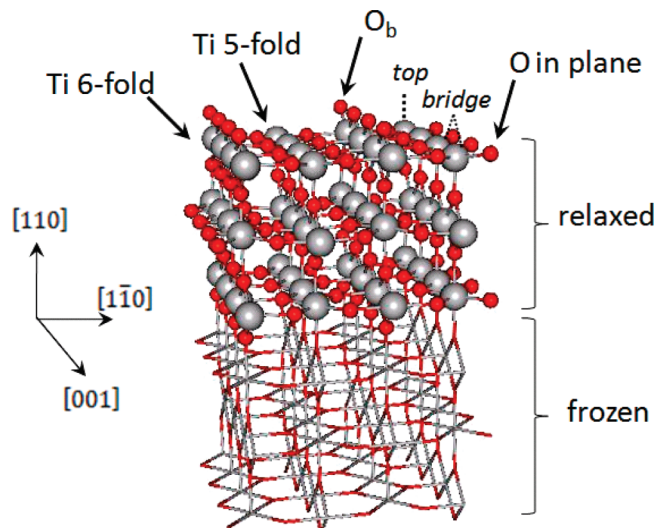


Figure 1. 4 × 2 supercell model of a TiO₂ (110) surface with six O–Ti–O layers; the three lower layers are kept frozen and the three upper layers are fully optimized. Atom colors: red = O, gray = Ti.

of molecularly adsorbed O₂ species that are not involved in vacancy oxidation, but are stabilized on the surface through interaction with Ti cations.¹⁹

The surface chemistry and photochemistry of organic compounds on the TiO₂ surface is a topic of recurrent interest in the literature. In particular, acetone has been the subject of diverse studies.^{11,19–27} Acetone photodecomposition is of particular importance because it is commonly found as a volatile contaminant, aside from being present either as reactant, intermediate, or product in many catalytic processes. The chemistry and photochemistry of acetone on the rutile TiO₂ (110) surface has been recently studied from a experimental viewpoint by Henderson.^{19–24}

* Corresponding author. E-mail: marquez@us.es.

In one of these studies,²⁴ the interaction of acetone with oxidized and reduced surfaces of TiO₂ (110) was examined using TPD, low-energy electron diffraction (LEED), oxygen isotope exchange, and high-resolution electron energy-loss spectroscopy (HREELS). TPD data indicate strong coverage dependence in the binding energy of acetone tentatively ascribed to the presence of acetone–acetone steric repulsions. At the reduced surface, no TPD state associated with vacancies and no acetone decomposition products are observed in contrast with the general impression about the dominant role of vacancies in determining the reactivity of the rutile TiO₂ (110) surface.^{1,5} However, TPD data for acetone desorption at the oxidized surface shows that the presence of a reactive oxygen species at this surface enhances acetone binding and also induces the formation of some acetone/oxygen complex that results in detectable acetone decomposition. The level of decomposition is found to be equivalent to the previous vacancy coverage and, thus, is linked to the formation of reactive oxygen species at the surface as the result of the interaction of molecular oxygen with vacancies. It is also proposed in this paper²⁴ that the presence of oxygen at the surface also stabilizes acetone–surface binding by reducing acetone–acetone lateral interactions.

This work focuses on understanding and rationalizing, at a microscopic level, the energetics and adsorption geometries of acetone on the rutile TiO₂ (110) surface. After presenting some technical details about the models and methodology applied, we will start by examining the adsorption process at the ideal, stoichiometric surface. The energetics, adsorption geometries, and coverage effects will be studied first on this ideal surface to separate any effects that may be induced by the presence of vacancies or by the degree of oxidation of the surface. Later, the adsorption at the reduced surface will be studied by using different supercell models that will simulate different degrees of surface reduction. Finally, the adsorption at the oxidized surface will be examined by using different models that take into account the simultaneous presence of oxygen, both as an O₂ molecule healing a vacancy and as an O-adatom at the channel, that may interact and modify the acetone adsorption process. In the final section we will establish the conclusions from our work.

Surface and Computational Model

In order to model the extended nature of these surfaces, periodic three-dimensional DFT calculations were carried out using the VASP 4.6 code^{28–30} with the projector augmented wave (PAW) method.^{31,32} In these calculations, the energy was obtained using the generalized gradient approximation (GGA) implementation of DFT proposed by Perdew et al.³³ and the electronic states were expanded using plane wave basis set with a cutoff of 400 eV. Forces on the ions were calculated through the Hellmann–Feynman theorem as the partial derivatives of free energy with respect to the atomic coordinates, including the Harris–Foulkes correction to forces.³⁴ This calculation of the force allows a geometry optimization using the conjugated gradient scheme. Iterative relaxation of the atomic positions was stopped when the forces on the atoms were less than 0.05 eV/Å. Desorption barriers have been located by using the climbing image version of the nudged elastic band algorithm.³⁵ In order to analyze the charge transfer upon adsorption, we have determined the total charge of the acetone molecule using the algorithm introduced by Henkelman et al.^{36,37} for the evaluation of the Bader charges.³⁸

For the calculations presented in this paper, slab models of different sizes and adequate thickness are used to represent the

TiO₂ (110) surface. It is known⁷ that vacancy formation energies based on slab calculations show an oscillant behavior with the number of layers and that at least six TiO₂ layers are required to obtain fully converged values. In the present work, we used supercell models with four and six TiO₂ layers to represent the TiO₂ (110) surface and explore the energetics and geometries of adsorption of acetone on this surface. Each slab was separated by a vacuum of 10 Å, considered enough to avoid interaction between the slabs.⁷ In all cases, the optimized lattice parameters for the bulk used were $a = 4.616 \text{ \AA}$, $c = 2.974 \text{ \AA}$, and $u = 0.304 \text{ \AA}$. The a and c parameters were kept fixed during the surface atomic positions relaxation. Multiples of the unit cell along the [001] direction give cells of the $n \times 1$ type and doubling along the [1̄1 0] direction gives $n \times 2$ cells. The surface cells that were used in the present work were 4×1 , where adsorption of a single acetone molecule represents a coverage of $\theta = 0.25$; 2×2 , where, again, adsorption of a single acetone molecule represents a coverage of $\theta = 0.25$; and, finally, a bigger cell of 4×2 size, where adsorption of a single acetone molecule represents a coverage of $\theta = 0.125$. The calculations for the 4×1 cells, were performed using the $2 \times 2 \times 1$ Monkhorst–Pack set of k -points,³⁹ those for the 2×2 supercell models used a $1 \times 2 \times 1$ Monkhorst–Pack set of k -points, while those corresponding to the bigger 4×2 supercell model where computed at the Γ point of the Brillouin zone.

To model the reduced TiO₂ (110) surface, one bridging oxygen atom has been removed from either the 4×1 or 4×2 supercell models. The 4×1 model represents a 25% vacancy concentration, much higher than typical concentrations of about 10% found experimentally.⁵ It has been shown that in this model, with vacancies separated by 6.6 Å, vacancy–vacancy interactions can be considered almost negligible.⁷ In our second set of models (those resulting from the 4×2 supercell), the vacancy concentration is 12.5%, much closer to typical experimental conditions and contains vacancies separated by 11.9 Å.

Desorption energies are always computed with respect to an isolated acetone molecule on a box of the same dimensions ($\text{BE} = E_{\text{surf}} + E_{\text{acetone}} - E_{\text{acetone/surf}}$). Thus, positive desorption energies represent bound states, stable with respect to desorption.

Results and Discussion

Stoichiometric Surface. Acetone adsorption on the regular TiO₂ (110) surface takes place by interaction of carbonyl group dipole with the surface electric field generated by the pentacoordinated Ti cations of the channels. Basically, thus, two high symmetry sites of adsorption can be expected on this surface: on top of the Ti cations of the channels and on a bridge position between two Ti cations. On each case, the acetone symmetry plane may be in different orientations with respect to the rows of bridging oxygens resulting in two limit conformations: with the acetone symmetry plane perpendicular to the bridging oxygen rows or parallel to them (see Figure 2).

The energetics of acetone adsorption on a 4×1 supercell model of the TiO₂ (110) regular surface, corresponding to a coverage of 0.25 ML is summarized in Table 1. Acetone adsorption takes place preferentially on the top site with a perpendicular orientation of the acetone symmetry plane relative to the bridging oxygen rows (η^1 -acetone) that allows for some additional stabilization through interaction between the acetone methyl groups and the protruding O anions. The binding energy is moderately strong (0.71–0.75 eV) and quite independent of the number of TiO₂ layers included in the model, indicating that a four-layer model may be enough to describe the relevant interactions in this system. It is also found that the acetone

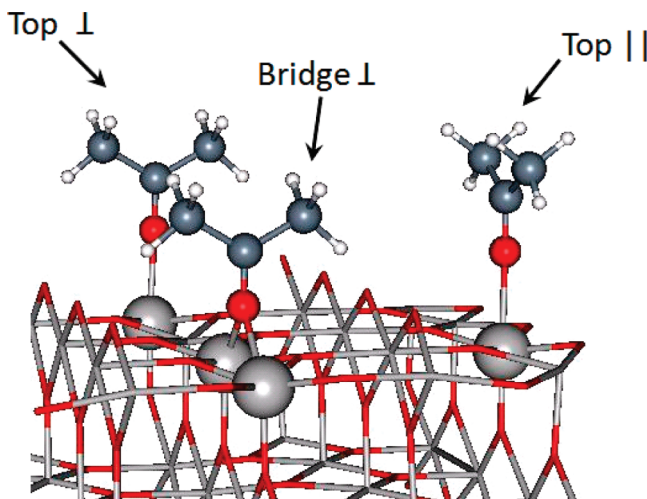


Figure 2. Adsorption sites and geometries for acetone on the regular TiO₂ (110) surface. Atom colors: red = O, gray = Ti, white = H, slate gray = C. ⊥: the acetone symmetry plane is perpendicular to the row of protruding oxygen atoms. ||: the acetone symmetry plane is parallel to the row of protruding oxygen atoms.

TABLE 1: Acetone Desorption Energies (D_e) on the Sites of a 4×1 Model of the TiO₂ (110) Stoichiometric Surface (0.25 ML)^a

site	D_e (eV)		
	number of TiO ₂ layers ^b		
	4 (2 + 2)	6 (2 + 4)	6 (3 + 3)
top	^c	0.65	0.67
	rot	0.72	0.73
	⊥	0.75	0.75
bridge		0.31	0.31
	⊥	0.34	0.35

^a See Figure 2 for a description of the sites. ^b (a + b) refers to the number of layers optimized (a) and frozen (b). ^c ||: the acetone symmetry plane is parallel to the rows of protruding oxygens. ⊥: the acetone symmetry plane is perpendicular to the rows of protruding oxygens. rot: the acetone symmetry plane is in an intermediate configuration.

molecule is practically free to rotate around the C–O axis, as the energy difference with the configuration where the acetone symmetry plane is parallel to the rows of protruding oxygens is only 0.1 eV. Adsorption on bridge sites is found to result in a weaker binding energy, about 0.32–0.35 eV. This means that translation of the acetone molecule through the Ti channels will be relatively hindered at low temperature, as it requires overcoming a barrier of at least 0.4 eV to jump from an on top position to the next one.

The distortion of the acetone molecule upon adsorption is small and quite similar for all sites, as shown by computed structural data. The carbonyl group (1.232–1.236 Å) slightly elongates when compared to the free acetone molecule (1.225 Å, computed in a 20 × 20 × 20 Å unit cell). This will indicate a small perturbation of the carbonyl bond upon adsorption that is also reflected in a weak displacement of the harmonic vibrational frequency toward lower wavenumbers: from 1716 cm⁻¹ in free acetone to 1684–1711 cm⁻¹ for the adsorbed molecule. Computation of the vibrational spectrum of the adsorbed acetone molecule show that both *top* and *bridge* sites lead to a minimum on the potential energy surface, but are very flat regarding the rotation of the acetone molecule or the internal rotation of the methyl groups.

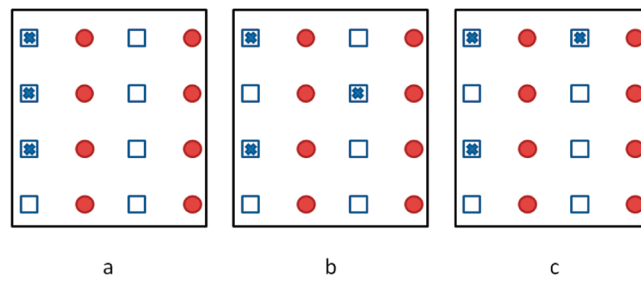
Experimental TPD data²⁴ for *d*₆-acetone shows, at coverages up to 0.5 ML, a prominent band that is asymmetric toward higher temperatures. At lower experimental coverage (0.12 ML), this band is centered at about 345 K on the reduced surface (375 K on the oxidized surface) and extends between 300 and 400 K. An important coverage dependence is observed on this TPD feature, quite evident by the shift of the leading edge toward lower temperature with increasing coverage, while the high temperature tail remains roughly unshifted. While this downward shift of the leading edge in the TPD spectrum has been tentatively assigned to the existence of acetone–acetone repulsions that destabilized acetone–surface binding,²⁴ our calculations allow for a different interpretation of this effect. Table 2 summarizes the dependence found between acetone loading and binding energies. In this Table, the energy required to go from a given initial surface coverage to a smaller one by removing one acetone molecule from the TiO₂ supercell models is presented for different surface coverages and different arrangements of the acetone molecules at the surface. The lower coverage computed (0.125 ML) corresponds to the binding of one acetone molecule in a 4 × 2 supercell model of the surface and is similar to the lower experimental coverage in the TPD spectrum (0.12 ML). The binding energy computed (0.87–0.92 eV) is in close agreement with the experimental data that, from the maximum of the TPD peak (345 K), estimated an apparent activation energy of 97 ± 6 kJ/mol (~1 eV). Increasing acetone loading to 0.250 ML results, on average, in lower binding energies: 0.71–0.75 eV when the final state corresponds to removal of all acetone molecules, as shown by the energies computed for the removal of the single acetone molecule present in the 4 × 1 and 2 × 2 supercell models. However, when we allow for having two distinct acetone molecules in the 4 × 2 supercell model, removal of a single acetone molecule results in a significantly lower binding energy of only 0.59–0.62 eV. This implies that the presence of some acetone coverage at the surface results in lower binding energies for the incoming acetone molecules, in agreement with the observed shift in the leading edge of the TPD spectrum with increasing coverage. However, in all these models, the distance between acetone molecules is never less than 4.2 Å along the channel, so some kind of steric repulsion cannot be invoked to explain the observed shift in the binding energy. Also, interaction between acetone molecules in nearby channels cannot be used as an argument, as the binding energies computed at this coverage for the 4 × 1 supercell model and for the 2 × 2 supercell model are basically the same, and in the later case there are no acetone molecules in the second channel. Indeed, the origin of the decrease in the acetone–TiO₂ (110) surface must be traced to the electronic properties of the system, concretely to the charge transfer that takes place upon adsorption of the acetone molecules. For the lower acetone loading (0.125 ML), a Bader charge analysis shows a net charge transfer of 0.14 e⁻ per acetone molecule from the acetone adlayer to the surface, mainly to the Ti 3d band, but very delocalized. The TiO₂ (110) surface thus gets partially reduced. When the coverage is increased to 0.250 ML, the amount of charge transfer per acetone molecule is smaller (0.10 e⁻), thus reducing the strength of the acetone–surface bond.

Using the 4 × 2 supercell model, a coverage of 0.375 ML can be simulated by placing three acetone molecules at the surface of the supercell model. Three different distributions of the acetone molecules are possible: in one of them, the three acetone molecule reside on the same channel, and in the other two configurations there are two acetone molecules in one

TABLE 2: Acetone Desorption Energies (D_e) from the On-Top Ti Site As Function of Total Acetone Loading and Distribution of Acetone Molecules on the Regular TiO_2 (110) Surface

coverage (ML)	# molecules per channel ^b	model	D_e (eV)		
			number of TiO_2 layers ^a		
			4 (2 + 2)	6 (2 + 4)	6 (3 + 3)
0.125	(1,0)	4 × 2	0.87	0.91	0.92
0.250	(1,1)	4 × 1	0.75	0.75	0.71
	(1,0)	2 × 2	0.74	0.75	0.73
	(2,0)	4 × 2	0.60	0.62	0.59
0.375	(3,0)	4 × 2	0.33	0.29	0.27
	(2,1)		0.60	0.56	0.53
			0.54	0.51	0.49
0.500	(1,1)	2 × 2	0.50	0.49	0.44
	(1,3)	4 × 2	0.45	0.44	0.37
			0.21	0.18	0.13
			0.24	0.24	0.19

^a ($a + b$) refers to number of layers optimized (a) and frozen (b). ^b Left: number of acetone molecules on the main channel (from where the acetone molecule is being desorbed). Right: number of acetone molecules on the neighboring channel.

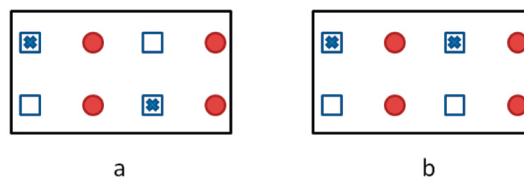
SCHEME 1: Possible Distributions of Three Acetone Molecules on the Surface of the 4×2 Supercell Model

● -bridging oxygens; □ fivefold coordinated Ti; ■ acetone molecule

channel and the last acetone molecule resides in the second channel (see Scheme 1).

In the latter two cases, desorption of the acetone molecule that resides on the least populated channel results in a binding energy of about 0.60–0.49 eV, similar to the energy required to remove one acetone molecule at a coverage of 0.250 ML, leaving behind another acetone molecule on the channel. This lower binding energy indicates that the electronic effects due to the partial electron transfer from the acetone adlayer to the surface propagate, although to a lesser extent, from one channel to the next. This is confirmed, again, by examination of the Bader atomic charges, which report an average transfer of 0.08 e⁻ per acetone molecule in this case (smaller than that for a 0.250 ML surface coverage) and 0.10 e⁻ for the acetone molecule in the least populated channel. While the absolute differences in the computed Bader charges are too small to give them a quantitative meaning, they show a definite trend of reducing charge transfer with increasing coverage. While the density of acetone molecules in one channel affects the binding properties of incoming molecules to neighboring channels, as discussed above, there is not a determinant influence that will make some Ti sites preferred over others that may produce an ordered acetone adlayer. When the two configurations **b** and **c** in Scheme 1 are compared, the difference in the computed binding energies is minimal (0.04–0.06 eV). The same can be said by examination of the binding energies reported for a coverage of 0.5 ML where, again, two different relative distributions of the acetone molecules are possible (see Scheme 2).

Binding energies are again reduced with increasing coverage due to a further reduction on the average amount of electron

SCHEME 2: Relative Configurations of Acetone Molecules for a Coverage of 0.5 ML on the 2×2 Supercell Model

● -bridging oxygens; □ fivefold coordinated Ti; ■ acetone molecule

transfer per acetone molecule to the TiO_2 (110) surface. However, the difference between the two configurations is minimal (0.05–0.07 eV). The absence of a local correlation between the relative positions of adsorbed acetone molecules in one channel and in nearby channels can be used to explain the lack of any high-order LEED patterns from the acetone adlayer at 0.5 ML found experimentally.²⁴

Further increase of the density of acetone molecules in a channel results in a situation where the incoming acetone molecule must occupy a Ti site in between two already occupied Ti sites. This configuration is sterically hindered as the methyl groups of adjacent acetone molecules come in close contact and must distort to allow for the newly adsorbed acetone molecule to penetrate the acetone adlayer and maximize its interaction with the TiO_2 surface. A direct consequence is that the binding energy of the incoming acetone molecule is drastically reduced: 0.27–0.33 eV for a 0.375 ML coverage and 0.13–0.21 eV for 0.5 ML coverage. This is in agreement with the development of a new, poorly resolved low temperature component in the TPD spectrum for coverages above 0.5 ML.²⁴

The results presented in this section have a neat interpretation: up to 0.5 ML there is a strong coverage dependence of the computed binding energy due to the partial surface reduction by the acetone molecules already present at the surface. However, a caveat must be introduced here to critically assess these results. Gradient corrected density functional theory has known limitations in the description of electronic defects due to inherent deficiencies in the functionals, mainly the insufficient cancellation of the self-interaction energy.⁴⁰ As result, the excess electron density provided by the incoming acetone molecules will be delocalized over the surface. The use of hybrid exchange–correlation functionals or the DFT+U approach, which adds an adjustable correction to enhance electron localization, allows one to overcome these deficiencies. As

TABLE 3: Acetone Desorption Energies (D_e) for a Single Acetone Molecule Per Unit Cell on the Vacant Site (v) and Channel Top Ti Sites (0, 1, and 2, Which Are, Respectively, First, Second, and Third Neighbors to the Vacancy) on 4 × 1 and 4 × 2 Supercell Models of the TiO₂ (110) Reduced Surface (See Figure 3 for a Description of the Adsorption Sites)^a

model	load (ML)	site	D_e (eV)		
			4 (2 + 2)	6 (2 + 4)	6 (3 + 3)
4 × 1	0.250	v	0.96	1.01	0.97
		0	0.59	0.61	0.59
		1	0.67	0.69	0.65
		2	0.65	0.66	0.64
4 × 2	0.125	v	1.03	1.07	1.10
		0	0.79	0.79	0.76
		1	0.82	0.83	0.83
		2	0.81	0.81	0.78

^a An oxygen vacancy is created on each model resulting in a 25% vacancy population on the 4 × 1 model and 12.5% vacancy population on the 4 × 2 model. Load is defined for this surface as the number of acetone molecules divided by the number of channel top Ti sites. ^b (a + b) refers to the number of layers optimized (a) and frozen (b).

recent studies on the electronic structure of defect states on TiO₂ (110) have shown,^{41,42} in either case the result is a localized character for single excess electrons in this surface. Extrapolation of these results to our case suggest that the strong coverage dependence found for the acetone binding energies will be attenuated to some point, but we can expect that, as far as adsorption properties and trends are concerned, there will be no qualitative changes that may require a new interpretation.

Reduced Surface. In Table 3, the computed binding energies for the adsorption of one acetone molecule on the vacancy and on regular Ti sites of the channels are presented. Acetone adsorption is enhanced at vacant sites of the reduced TiO₂ (110) surface when compared to the regular surface. Adsorption energies increase to 0.96–1.10 eV (compared to 0.87–0.92 eV, see Table 1) and are similar regardless of the supercell model used. The adsorption geometry of the acetone molecule at the vacant site is similar to the minimum geometry found on the regular Ti sites of the channels (see Figure 3), but with the acetone symmetry plane parallel to the rows of protruding O atoms and does not block adsorption of newly incoming acetone molecules on the pentacoordinated Ti sites of the channels. Data in Table 3 show that adsorption energies on these Ti channel sites are much affected by the degree of reduction of the surface. In the 4 × 1 supercell model, with an unrealistic 25% vacancy population, acetone binding energies are reduced to 0.59–0.69 eV. In the 4 × 2 supercell model, with a 12.5% vacancy population, much closer to experimental values, these binding energies increase to 0.79–0.83 eV, values closer to those found in the stoichiometric surface. These results indicate that, while the properties of the vacant site may be correctly reproduced by small supercell models, high degrees of surface reduction will affect the properties of the regular channel sites, resulting in an incorrect behavior of the models.

Oxidized Surface. The chemistry of the oxidized TiO₂ (110) surface has proved to be quite complex and, following the latest developments, involves both atomic and molecular forms of oxygen at the surface. The main channel to the surface oxidation implies the adsorption of an O₂ molecule at a vacancy and its further dissociation to leave an O atom healing the vacancy and an O-adatom on the channel. Following those considerations

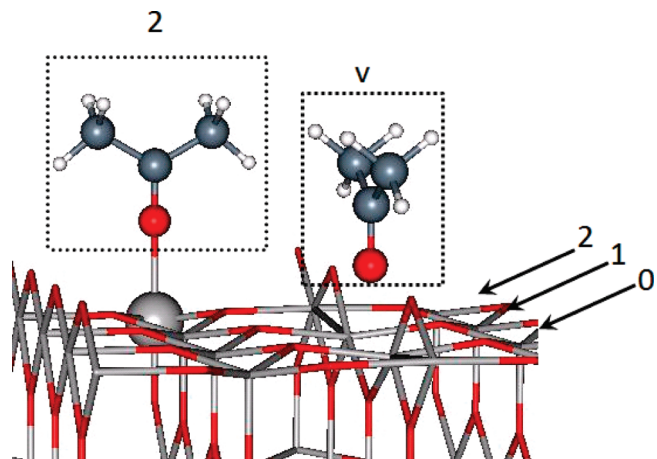


Figure 3: Adsorption sites and geometries for acetone on the reduced TiO₂ (110) surface. v: bridge-O vacancy site; 0, 1, and 2: regular pentacoordinated Ti channel sites that are, respectively, first, second, and third neighbors to the vacancy. Atom colors: red = O, gray = Ti, white = H, slate gray = C.

TABLE 4: Relative Energies for Molecular and Atomic Forms of Oxygen on a 4 × 2 Supercell Model of the TiO₂ (110) Surface

site and orientation ^a	relative energies (eV)		
	4 (2 + 2)	6 (2 + 4)	6 (3 + 3)
O ₂ /vac	⊥ to row	0.13	0.11
	to row	0.90	0.87
	vertical	1.28	1.28
O ₂ /channels	top	0.96	0.95
	bridge	0.00	0.00

^a The symbols ⊥, ||, and the word “vertical” indicate the orientation of the axis of the O₂ molecule that occupies the vacancy relative to the row of protruding oxygen atoms.

different conformations of an O₂ molecule at a vacancy and of an O-adatom at the channel have been optimized on a 4 × 2 supercell model and their relative energies are presented in Table 4. In agreement with previous findings^{43,44} both forms are nearly degenerate. The O₂ molecule at the vacancy prefers to be parallel to the surface with the molecular axis perpendicular to the row of protruding oxygen atoms. The large computed O–O equilibrium bond length (1.43 Å) reveals a strong interaction with the vacancy that suggest a strong charge transfer toward the O₂ molecule. When the oxidized surface is modeled by adding an oxygen atom to the channel, the resulting configuration, where this O-adatom has a bond distance of 1.46 Å to one basal atom, is slightly preferred by 0.1 eV, indicating that a strong interaction should also exist in this case.

Experimental TPD data²⁴ for *d*₆-acetone adsorption on a oxygen precovered TiO₂ (110) reduced surface results in both stabilization and detectable decomposition. The low-coverage feature found at 345 K on the reduced surface is shifted to 375 K on the oxidized surface and shows a more symmetric profile. On the basis of oxygen isotope exchange studies, this TPD feature is assigned to some form of acetone–surface oxygen complex with an apparent activation energy of 105 ± 7 kJ/mol that, upon heating, reversibly liberates acetone from the surface.

Table 5 presents the binding energies computed for the adsorption of a single acetone molecule at the different sites (see Figure 4 for a description) of the 4 × 2 supercell model of the oxidized TiO₂ (110) surface. Only the binding energies computed for the most stable configuration (with the acetone symmetry plane perpendicular to the rows of protruding

TABLE 5: Acetone Desorption Energies (D_e) for Single Acetone Molecule Channel Top Ti Sites on the Two 4×2 Supercell Models of the Oxidized TiO_2 (110) Surface (See Figure 4 for a Description of the Adsorption Sites)^b

model	site	D_e (eV)		
		number of TiO_2 layers ^a	4 (2 + 2)	6 (2 + 4)
O/channel	0	0.70	0.75	0.71
	1	0.83	0.85	0.82
	c0	0.84	0.86	0.82
	c1	0.85	0.87	0.82
O_2/vac	0	0.75	0.76	0.83
	1	0.84	0.86	0.91
	2	0.83	0.85	0.90

^a On the O/channel model, **0** and **1** denote sites that are first and second neighbors to the O adatoms; **c0** and **c1** denote the two nonequivalent top Ti sites on the channel that do not have an O adatom. On the O_2/vac model, **0**, **1**, and **2** denote top Ti sites that are, respectively, first, second, and third neighbors to the O_2 molecule that is healing the vacancy. ^b (*a* + *b*) refers to number of layers optimized (*a*) and frozen (*b*).

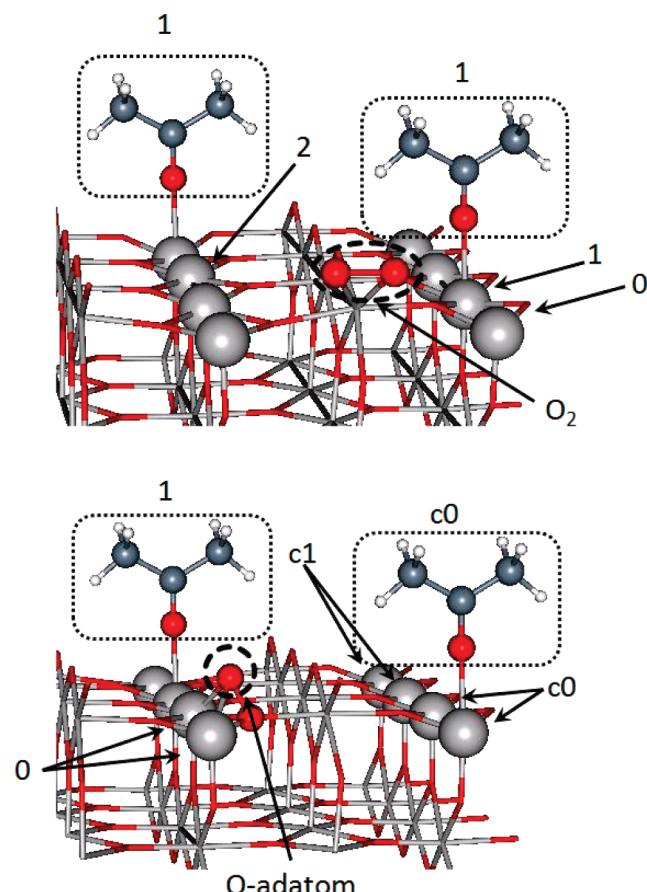


Figure 4. Adsorption sites and geometries for acetone on the oxidized TiO_2 (110) surface. Top: 4×2 supercell model with an O_2 molecule healing a bridge-O vacancy; **0**, **1**, **2**: regular pentacoordinated Ti sites that are, respectively, first, second, and third neighbors to the molecule. Bottom: 4×2 supercell model with an O adatom on one of the channels; **0** refers to atoms bonded to the O adatom; **1** refers to the first-neighbor Ti atom; **c0** and **c1** refer to pentacoordinated Ti atoms on the channel free of O adatoms. Atom colors: red = O, gray = Ti, white = H, slate gray = C.

oxygens) are reported. When the additional oxygen is in the form of an O-adatom, binding energies lie in the 0.82–0.87 eV range, values similar to those found on the regular sites of the stoichiometric surface (see Table 2), if the acetone molecule

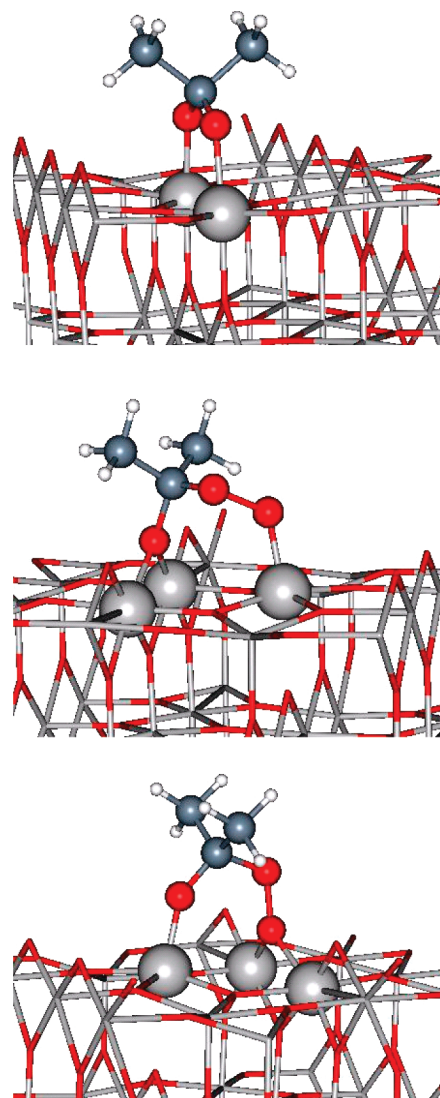


Figure 5. Adsorption geometries for acetone/O-adatom complexes (1-top, 2-middle, 3-bottom) on the TiO_2 (110) surface. Atom colors: red = O, gray = Ti, white = H, slate gray = C.

binds to a Ti atom not directly interacting with the surface O-adatom. If the acetone molecule binds to one of the Ti atoms interacting with the O-adatom, the acetone–surface interaction gets destabilized, resulting in a lower binding energy (0.70–0.75 eV). When the additional oxygen is in the form of one O_2 molecule filling a vacancy, the behavior is similar. Adsorption at Ti sites not in close contact with the O_2 molecule results in binding energies in the 0.83–0.91 eV range, close to those found for adsorption on the pentacoordinated Ti sites of the stoichiometric surface. Adsorption on the Ti cation that is first neighbor to the preadsorbed O_2 molecule is only slightly weaker (0.75–0.83 eV) in this case. These data are clearly inconsistent with the available experimental information implying that η^1 -acetone cannot be made responsible for the low coverage TPD feature found at higher temperatures. Trying to find some form of acetone/O-adatom complex that may stabilize acetone at the surface and that reversibly liberates acetone upon heating, the three complexes depicted in Figure 5 have been found. Computed desorption energies for acetone from these three complexes in a 4×2 supercell model of the oxidized TiO_2 (110) surface are presented in Table 6. In all cases, acetone desorption from these complexes may result in O exchange between acetone and the surface, in agreement with $^{16}\text{O}/^{18}\text{O}$

TABLE 6: Acetone Desorption Energies and Energetic Desorption Barriers on a 4 × 2 Supercell Model of the Oxidized TiO₂ (110) Surface (See Figure 5 for a Description of the Adsorption Sites)

model	D _e (eV)			ΔE _{desorp} [‡] (eV)
	4 (2 + 2)	6 (2 + 4)	6 (3 + 3)	
1	0.82	0.84	0.79	1.31
2	0.78	0.84	0.80	1.02
3	0.72	0.70	0.67	1.84

isotope exchange studies.²⁴ Acetone desorption energies from these complexes are in the 0.67–0.84 eV range, and thus are similar to those found for the desorption of η^1 -acetone from this surface, and do not explain the experimental data. Nevertheless, one has to remember that the analysis of the TPD data yields the apparent *activation energy* for the desorption process. Computation of minimum energy paths (MEPs) for the acetone desorption process show that, while for η^1 -acetone complexes the process is barrier free, this is not the case for the three acetone/O-adatom complexes depicted in Figure 5. After characterizing the maximum at these MEPs as true transition states (TSs), the energetic barrier for the acetone desorption process has been computed as the energy difference between the TS and the precursor state. These barriers are presented also in Table 6. Disregarding results for complex **3**, which shows lower stability than complexes **1** and **2** and presents a high desorption barrier, apparent activation energies for the acetone desorption process will lie in the 1.0–1.3 eV range, in agreement with the experimental value of 105 ± 7 kJ/mol obtained from the analysis of the TPD feature found at 375 K.²⁴ Thus, coadsorbed oxygen stabilizes acetone via the formation of acetone/O-adatom complexes that, in contrast to η^1 -acetone, present a barrier for desorption. This barrier allows us to explain the high temperature feature observed in the TPD spectrum for acetone desorption from the oxidized TiO₂ (110) surface. At higher acetone loadings, experimental data²⁴ suggest the presence of a polyacetone complex at the Ti channels of the TiO₂ (110) surface that could be made responsible for this high-temperature TPD feature. However, our calculations seem to rule out this possibility. A surface biacetone complex obtained by coordination of two adsorbed acetone molecules linked through an O-adatom is found to be unstable with respect to dissociation on an adsorbed diolate and an η^1 -acetone by 1.4 eV. So, energetically the formation of poly acetone complexes at the TiO₂ (110) surface is unlikely.

Conclusions

In the present work a systematic study of the adsorption of acetone at the TiO₂ (110) surface has been carried out by means of plane-wave pseudopotential DFT calculations. The computed desorption energy for η^1 -acetone from the TiO₂ (110) stoichiometric surface channels is in close agreement with experimental data. The observed dependence between the surface acetone loading and the maximum of the TPD peak is explained on the basis of the bonding mechanism that, based on a Bader charge analysis, implies some degree of surface reduction by the acetone molecule. This partial surface reduction results in a smaller interaction with newly incoming acetone molecules, resulting in a lower binding energy with increasing acetone loading. The effect is purely electronic, as there is no contribution of acetone–acetone lateral repulsions, as acetone molecules, up to a coverage of 0.5 ML, are at least 4.2 Å apart. Although limitations in the PW91 functional result in an excessive

delocalization of the charge transferred from the acetone molecules to the surface, it is not expected that a more accurate functional (like hybrid exchange–correlation functionals or the DFT+U method) will qualitatively change the trends found in the acetone binding energies. A more localized description of the surface excess electron density may result in a lower coverage dependence of the acetone desorption energies but, unless the bonding mechanism is altered, the trends found will be qualitatively preserved. It is also found that there is no correlation between the adsorption of acetone molecules on nearby channels, in agreement with the lack of any high-order LEED patterns (other than the 1 × 1) from the acetone adlayer. Adsorption at bridge oxygen vacancies does not result in a stronger interaction between the acetone molecule and the surface when compared with the adsorption at the pentacoordinated Ti atoms from the channels. The minimum geometry found indicates also that adsorption at vacancy sites does not block adsorption at the channels. The binding of the acetone molecule to the pentacoordinated Ti sites of the channels is found to be highly dependent on the number of bridge oxygen vacancies generated in the surface model. The presence of vacancies results in a reduction of the surface that, in turn, reduces the binding energy of the acetone to the TiO₂ (110) surface. This result is of especial importance in the development of models to study the reactivity of this surface, as it shows that supercell models with a degree of reduction higher than those found experimentally (7–10% vacancy population) will result in an incorrect description of the adsorbate/surface interaction; however, they may correctly reproduce the interaction with vacancy sites. Binding energies for η^1 -acetone adsorption on models of the oxidized TiO₂ (110) surface are similar to those found on the regular sites of the stoichiometric surface in contrast with experimental data that indicate a stabilization of acetone at this oxidized surface. The formation of acetone/O-adatom complexes that develop a barrier for acetone desorption allows us to explain the high temperature feature observed in the experimental TPD spectrum.

Acknowledgment. This work was funded by the Spanish Ministerio de Educación y Ciencia, MEC (project MAT2008-04918) and the Junta de Andalucía (project P08-FQM-03661). Part of the computer time was provided by the Centro Informático Científico de Andalucía (CICA). This work has benefited from the support of COST Action D37 (“GridChem”).

References and Notes

- (1) Henrich, V.; Cox, P. *The Surface Science of Metal Oxides*; Cambridge University Press: Cambridge, UK, 1994.
- (2) Thomson, T.; Yates, J. T. *Chem. Rev.* **2006**, *106*, 4428–4453.
- (3) Linsebigler, A. L.; Lu, G.; Yates, J. T. *Chem. Rev.* **1995**, *95*, 735–758.
- (4) Henry, C. R. *Surf. Sci. Rep.* **1998**, *31*, 231–325.
- (5) Diebold, U. *Surf. Sci. Rep.* **2003**, *48*, 53–229.
- (6) Diebold, U.; Lehman, J.; Mahmoud, T.; Kuhn, M.; Leonardelli, G.; Hebenstreit, W.; Schmid, M.; Varga, P. *Surf. Sci.* **1998**, *411*, 137–153.
- (7) Oviedo, J.; Miguel, M. A. S.; Sanz, J. F. *J. Chem. Phys.* **2004**, *121*, 7427–7433.
- (8) Han, P.; Goodman, D. W. *J. Phys. Chem. C* **2008**, *112*, 6390–6397.
- (9) Schaub, R.; Thostrup, P.; López, N.; Lægsgaard, E.; Stensgaard, I.; Nørskov, J. K.; Besenbacher, F. *Phys. Rev. Lett.* **2001**, *87*, 266104.
- (10) Schaub, R.; Wahlström, E.; Rønnaug, A.; Lægsgaard, E.; Stensgaard, I.; Besenbacher, F. *Science* **2003**, *299*, 377–379.
- (11) Fujishima, A.; Zhang, X.; Tryk, D. A. *Surf. Sci. Rep.* **2008**, *63*, 515–582.
- (12) Du, Y.; Dohnálek, Z.; Lyubinetsky, I. *J. Phys. Chem. C* **2008**, *112*, 2649–2653.
- (13) Epling, W. S.; Peden, C. H. F.; Henderson, M. A.; Diebold, U. *Surf. Sci.* **1998**, *412–413*, 333–343.

- (14) Henderson, M. A.; Epling, W. S.; Perkins, C. L.; Peden, C. H. F.; Diebold, U. *J. Phys. Chem. B* **1999**, *103*, 5328–5337.
- (15) Du, Y.; Deskins, N. A.; Zhang, Z.; Dohnálek, Z.; Dupuis, M.; Lyubinetsky, I. *J. Phys. Chem. C* **2009**, *113*, 666–671.
- (16) Zhang, Z.; Du, Y.; Petrik, N. G.; Kimmel, G. A.; Lyubinetsky, I.; Dohnálek, Z. *J. Phys. Chem. C* **2009**, *113*, 1908–1916.
- (17) Wendt, S.; Schaub, R.; Matthesen, J.; Vestergaard, E.; Wahlström, E.; Rasmussen, M.; Thstrup, P.; Molina, L.; Lægsgaard, E.; Stensgaard, I.; Hammer, B.; Besenbacher, F. *Surf. Sci.* **2005**, *598*, 226–245.
- (18) Wendt, S.; Matthesen, J.; Schaub, R.; Vestergaard, E. K.; Lægsgaard, E.; Besenbacher, F.; Hammer, B. *Phys. Rev. Lett.* **2006**, *96*, 066107.
- (19) Henderson, M. *J. Phys. Chem. C* **2008**, *112*, 11433–11440.
- (20) Henderson, M. A. *J. Catal.* **2008**, *256*, 287–292.
- (21) Henderson, M. A. *J. Phys. Chem. B* **2005**, *109*, 12062–12070.
- (22) Henderson, M. A. *Langmuir* **2005**, *21*, 3443–3450.
- (23) Henderson, M. A. *Langmuir* **2005**, *21*, 3451–3458.
- (24) Henderson, M. A. *J. Phys. Chem. B* **2004**, *108*, 18932–18941.
- (25) Coronado, J. M.; Zorn, M. E.; Tejedor-Tejedor, I.; Anderson, M. A. *Appl. Catal. B: Environ.* **2003**, *43*, 329–344.
- (26) El-Maazawi, M.; Finken, A. N.; Nair, A. B.; Grassian, V. H. *J. Catal.* **2000**, *191*, 138–146.
- (27) Carter, E.; Carley, A. F.; Murphy, D. M. *ChemPhysChem* **2007**, *8*, 113–123.
- (28) Kresse, G.; Hafner, J. *Phys. Rev. B* **1996**, *47*, 558–561.
- (29) Kresse, G.; Furthmüller, J. *Comput. Mater. Sci.* **1996**, *6*, 15.
- (30) Kresse, G.; Furthmüller, J. *Phys. Rev. B* **1996**, *54*, 11169–11186.
- (31) Blöchl, P. E. *Phys. Rev. B* **1994**, *50*, 17953–17979.
- (32) Kresse, G.; Joubert, D. *Phys. Rev. B* **1999**, *59*, 1758–1775.
- (33) Perdew, J. P.; Chevary, J. A.; Vosko, S. H.; Jackson, K. A.; Pederson, M. R.; Singh, D. J.; Fiolhais, C. *Phys. Rev. B* **1992**, *46*, 6671–6687.
- (34) Harris, J. *Phys. Rev. B* **1985**, *31*, 1770–1779.
- (35) Henkelman, G.; Uberuaga, B. P.; Jonsson, H. *J. Chem. Phys.* **2000**, *113*, 9901–9904.
- (36) Henkelman, G.; Arnaldsson, A.; Jonsson, H. *Comput. Mater. Sci.* **2006**, *36*, 354–360.
- (37) Sanville, E.; Kenny, S. D.; Smith, R.; Henkelman, G. *J. Comput. Chem.* **2007**, *28*, 899–908.
- (38) Bader, R. *Atoms in Molecules: A Quantum Theory*; Oxford University Press: Oxford, U.K., 1990.
- (39) Monkhorst, H. J.; Pack, J. D. *Phys. Rev. B* **1976**, *13*, 5188–5192.
- (40) Koch, W.; Holthausen, M. C. *A Chemist Guide to Density Functional Theory*; Wiley-VCH: Weinheim, Germany, 2002.
- (41) Valentin, C. D.; Pacchioni, G.; Selloni, A. *Phys. Rev. Lett.* **2006**, *97*, 166803.
- (42) Deskins, N. A.; Rousseau, R.; Dupuis, M. *J. Phys. Chem. C* **2009**, *113*, 14583–14586.
- (43) Rasmussen, M. D.; Molina, L. M.; Hammer, B. *J. Chem. Phys.* **2004**, *120*, 988–997.
- (44) Tilocca, A.; Selloni, A. *ChemPhysChem* **2005**, *6*, 1911–1916.

JP906643H